ACADEMIC PRESS

Available online at www.sciencedirect.com

SCIENCE DIRECT®

Journal of Solid State Chemistry 174 (2003) 441–449

JOURNAL OF SOLID STATE CHEMISTRY

http://elsevier.com/locate/jssc

New alkali–metal–molybdenum(VI)–selenium(IV) oxides: syntheses, structures, and characterization of A_2SeMoO_6 ($A = Na^+$, K^+, or Rb^+)☆

Yetta Porter and P. Shiv Halasyamani*

Department of Chemistry, Center for Materials Chemistry, University of Houston, 136 Fleming Building, Houston, TX 77204-5003, USA

Received 27 February 2003; received in revised form 9 May 2003; accepted 17 May 2003

Abstract

Three new quaternary selenites, A_2SeMoO_6 ($A = Na^+$, K^+, or Rb^+), were synthesized through the solid-state reaction of A_2MoO_4 with SeO_2 at 400°C. Although the reported materials are 'stoichiometrically equivalent', the compounds exhibit strikingly different crystal structures. Whereas Na_2SeMoO_6 has a three-dimensional crystal structure, K_2SeMoO_6 and Rb_2SeMoO_6 are molecular and uni-dimensional, respectively. However, all of the new materials have structures containing Mo^{6+} octahedra linked to Se^{4+} trigonal pyramids. Although the Mo^{6+} and Se^{4+} cations are in local asymmetric environments in all three materials, only Na_2SeMoO_6 is non-centrosymmetric. Single crystal X-ray data: Na_2SeMoO_6, cubic, space group, $P2_13$ (no. 198), $a = 8.375(5)$ Å, $Z = 4$, $R(F) = 0.0143$; K_2SeMoO_6, monoclinic, space group, $P2_1/c$ (no. 14), $a = 6.118(8)$ Å, $b = 15.395(2)$ Å, $c = 7.580(9)$ Å, $\beta = 112.39(4)^\circ$, $Z = 4$, $R(F) = 0.0281$; Rb_2SeMoO_6, orthorhombic, space group, $Pnma$ (no. 62), $a = 7.805(9)$ Å, $b = 6.188(7)$ Å, $c = 14.405(4)$ Å, $Z = 4$, $R(F) = 0.0443$.

Keywords: Synthesis; Mixed-metal oxides; Second-harmonic generation; Crystal structure

1. Introduction

Cations with stereo-active lone pairs, e.g., Sn^{2+}, Se^{4+}, and Te^{4+}, are of interest owing to their variable coordination environment, rich structural chemistry, and interesting physical properties [1–5]. The occurrence of the lone pair has been attributed to second-order Jahn–Teller (SOJT) effects [6–16]. Usually, these cations are bonded to three to seven oxide ligands in an asymmetric coordination environment attributable to their stereo-active lone pair. With respect to mixed-metal Se^{4+} oxides, a number of materials have been reported [17–25]. Common to all these compounds is the asymmetric $(SeO_3)^{2-}$ group. We are interested in synthesizing new materials that contain Se^{4+} and other d^0 transition metal cations, e.g., Nb^{5+}, Mo^{6+}, and W^{6+}, in order to combine SOJT distorted cations. Our goal is to use the local asymmetric environment created by the SOJT distortion towards the 'rational design' of new non-centrosymmetric (NCS) materials. Recently, we have synthesized several new oxides containing both d^0 transition metals and cations with stereo-active lone pairs [26–30], and demonstrated that some of these new materials have substantial SHG responses [28–30]. The large SHG responses can be attributed to the constructive addition of the individual bond hyperpolarizabilities. With respect to Se^{4+}–Mo^{6+} oxides, a few materials have been reported [31–35], some of which are NCS [34,35]. We report in this paper the syntheses, structures, and characterization of three new materials, A_2SeMoO_6 ($A = Na^+$, K^+, or Rb^+). Although both the Mo^{6+} and Se^{4+} cations are in distorted coordination environments, only Na_2SeMoO_6 is NCS.

☆Further details of the crystal structure investigations can be obtained from the Fachinformationszentrum Karlsruhe, 76344 Eggenstein-Leopoldshafen, Germany, (fax: (49) 7247-808-666; e-mail: crysdata@fiz.karlsruhe.de) on quoting the depository numbers CSD-412998 for Na_2SeMoO_6, CSD-412999 for K_2SeMoO_6 and CSD-413000 for Rb_2SeMoO_6.

*Corresponding author. Fax: +1-713-743-2787.

E-mail address: psh@uh.edu (P.S. Halasyamani).

0022-4596/03/$ - see front matter © 2003 Elsevier Inc. All rights reserved.
doi:10.1016/S0022-4596(03)00296-2

2. Experimental

2.1. Reagents

SeO_2 (99.4%, Alfa Aesar), MoO_3 (99.5%, Fluka), $Na_2MoO_4 \cdot 2H_2O$ (99.5%, Alfa Aesar), and $K_2MoO_4 \cdot 2H_2O$ (98.9%, Fluka) were used as received. $Na_2MoO_4 \cdot 2H_2O$ and $K_2MoO_4 \cdot 2H_2O$ were dehydrated by heating the powders in air to 250°C for 15 h to produce Na_2MoO_4 and K_2MoO_4. Rb_2MoO_4 was synthesized through a solid-state reaction of polycrystalline Rb_2CO_3 and MoO_3 that was heated in air to 550°C for 1 day, and then quenched to room temperature. The purity and anhydrous nature of the A_2MoO_4 ($A = Na^+$, K^+, or Rb^+) oxides were confirmed by powder X-ray diffraction and thermogravimetric analysis.

2.2. Synthesis

All the reported materials were synthesized from stoichiometric amounts of SeO_2 and A_2MoO_4 ($A = Na^+$, K^+, or Rb^+). The powder reagents were ground together and pressed into a 1 cm pellet. The pellets were placed into separate fused silica tubes that were subsequently evacuated and sealed. The tubes were heated to 370°C for 1 day and cooled at 6°C/h to ambient temperature. All three materials were synthesized as colorless polycrystalline powders along with clear colorless crystals. The yields for Na_2SeMoO_6 and K_2SeMoO_6 were over 90% based on A_2MoO_4 ($A = Na^+$ or K^+). In all instances, some of the product adhered to the inside of the quartz tube. The K-product is moderately air stable, with decomposition occurring over several days. The Rb-product was shown to be air and moisture sensitive, thus the tube was opened in a nitrogen-filled glove bag. All three materials are unstable in water. In addition, for all three materials, single crystals were manually extracted from the powder.

2.3. Crystallographic determination

The structures of A_2SeMoO_6 ($A = Na^+$, K^+, or Rb^+) were determined by standard crystallographic methods. For all three materials clear, colorless faceted crystals were used. Crystal size: Na_2SeMoO_6 ($0.05 \times 0.08 \times 0.20\,mm^3$), K_2SeMoO_6 ($0.06 \times 0.15 \times 0.25\,mm^3$), Rb_2SeMoO_6 ($0.02 \times 0.04 \times 0.30\,mm^3$). Room temperature intensity data were collected on a Siemens SMART diffractometer equipped with a 1 K CCD area detector using graphite monochromated MoKα radiation. A hemisphere of data was collected up to 56° in 2θ using a narrow-frame method with scan widths of 0.30° in omega and an exposure time of 25 s/frame. The first 50 frames were remeasured at the end of the data collection to monitor instrument and crystal stability. The maximum correction applied to the intensities was <1%. The data were integrated using the Siemens SAINT program [36], with the intensities corrected for Lorentz, polarization, air absorption, and absorption attributable to the variation in path length through the detector faceplate. Psi-scans were used for the absorption correction on the hemisphere of data. The phase problem was solved using SHELXS-97 [37] and the data refined using SHELXL-97 [38]. All atoms were refined with anisotropic thermal parameters. The refinements converged for $I > 2\sigma(I)$, and all calculations were performed using the WinGX-98 crystallographic software package [39]. Crystallographic data, atomic coordinates, equivalent displacement parameters, and selected bond distances and bond angles are given in Tables 1–5.

Table 1
Crystallographic data for Na_2SeMoO_6, K_2SeMoO_6, and Rb_2SeMoO_6

Chemical formula	Na_2SeMoO_6	K_2SeMoO_6	Rb_2SeMoO_6
Formula weight	316.88	349.10	441.84
Space group	$P2_13$ (no. 198)	$P2_1/c$ (no. 14)	$Pnma$ (no. 62)
T (K)	293.0(2)	293.0(2)	293.0(2)
λ (Å)	0.71073	0.71073	0.71073
ρ_{calc} (g/cm^3)	3.583	3.512	4.217
μ (cm^{-1})	85.37	87.27	209.83
a (Å)	8.375(5)	6.118(8)	7.805(9)
b (Å)	8.375(5)	15.395(2)	6.188(7)
c (Å)	8.375(5)	7.5809(9)	14.405(2)
α (deg)	90	90	90
β (deg)	90	112.39(1)	90
γ (deg)	90	90	90
V (Å^3)	587.41(6)	660.26(13)	695.90(13)
Z	4	4	4
Reflections	3547	3924	4000
Unique data	474	1483	880
$I > 2\sigma(I)$	462	1384	750
Parameters	32	92	56
Flack parameter	0.003(13)	N/A	N/A
$R(F)$, $R_w(F^2)$	0.0143, 0.0368	0.0281, 0.0702	0.0443, 0.0969

$R = \sum||F_o|-|F_c||/\sum|F_o|$; $R_w = [\sum w(F_o^2-F_c^2)^2/\sum w(F_o^2)^2]^{1/2}$.

Table 2
Atomic coordinates and equivalent displacement parameters for Na_2SeMoO_6

Atom	x	y	z	U_{eq} (Å)
Na(1)	0.0320(1)	0.5320(1)	−0.0320(1)	0.022(1)
Na(2)	0.7501(1)	0.2499(1)	−0.2501(1)	0.023(1)
Mo(1)	0.5073(1)	0.4927(1)	−0.0073(1)	0.011(1)
Se(1)	0.8273(1)	0.3273(1)	0.1727(1)	0.011(1)
O(1)	0.9016(2)	0.5024(2)	0.2447(2)	0.015(1)
O(2)	0.3106(2)	0.5147(2)	−0.0759(2)	0.021(1)

U_{eq} is defined as one-third of the trace of the orthogonalized U_{ij} tensor.

Table 3
Atomic coordinates and equivalent displacement parameters for K_2SeMoO_6

Atom	x	y	z	U_{eq} (Å)
K(1)	0.6432(2)	0.1994(1)	0.3896(1)	0.026(1)
K(2)	0.1104(2)	0.4426(1)	−0.1889(1)	0.026(1)
Mo(1)	0.4596(1)	0.4381(1)	0.3142(1)	0.015(1)
Se(1)	0.1001(1)	0.3268(1)	0.3796(1)	0.018(1)
O(1)	0.1001(4)	0.3960(2)	0.1990(3)	0.020(1)
O(2)	0.3703(5)	0.5235(2)	0.1513(3)	0.025(1)
O(3)	0.7117(4)	0.4797(2)	0.5060(3)	0.021(1)
O(4)	0.5977(4)	0.6627(2)	0.5050(3)	0.020(1)
O(5)	0.5780(5)	0.3640(2)	0.2033(4)	0.025(1)
O(6)	0.0538(5)	0.2301(2)	0.2770(4)	0.033(1)

U_{eq} is defined as one-third of the trace of the orthogonalized U_{ij} tensor.

Table 4
Atomic coordinates and equivalent displacement parameters for Rb_2SeMoO_6

Atom	x	y	z	U_{eq} (Å)
Rb(1)	0.6565(1)	−0.2500	0.2999(1)	0.020(1)
Rb(2)	0.6285(1)	−0.2500	0.0329(1)	0.023(1)
Mo(1)	0.8973(1)	0.2500	0.2691(1)	0.012(1)
Se(1)	0.9166(1)	0.2500	0.0623(1)	0.018(1)
O(1)	0.6710(6)	0.2500	0.2764(4)	0.020(1)
O(2)	0.8889(4)	0.0484(5)	0.1429(3)	0.020(1)
O(3)	0.5492(5)	−0.0263(6)	−0.1647(2)	0.020(1)
O(4)	0.7431(7)	0.2500	−0.0028(4)	0.028(1)

U_{eq} is defined as one-third of the trace of the orthogonalized U_{ij} tensor.

2.4. Infrared spectroscopy

Infrared spectra were recorded on a Matteson FTIR 5000 spectrometer in the 400–4000 cm^{-1} range, with the sample pressed between two KBr pellets.

2.5. Thermogravimetric analysis

Thermogravimetric analyses were carried out on a TGA 2950 analyzer (TA instruments). The samples were contained within a platinum crucible and heated in air at a rate of $5°C\,min^{-1}$ to 800°C.

2.6. Second-order non-linear optical measurements

Powder SHG measurements were performed on a modified Kurtz-NLO [40] system using 1064 nm radiation. A detailed description of the equipment and the methodology used has been published [29]. No index matching fluid was used in any of the experiments. Powders with particle size in the range of 45–63 μm were used to compare SHG intensities.

3. Results and discussion

Although all three materials are ‘stoichiometrically equivalent’, each compound exhibits a strikingly different structural topology. Whereas Na_2SeMoO_6 has three-dimensional features, K_2SeMoO_6 and Rb_2SeMoO_6 have molecular and one-dimensional features, respectively. Na_2SeMoO_6 has cubic symmetry and contains MoO_6 octahedra linked to SeO_3 trigonal pyramids. Both cations are in asymmetric coordination environments attributable to SOJT distortions. The structure of Na_2SeMoO_6 may be described as consisting of eight-membered rings of alternating MoO_6 octahedra and SeO_3 groups that are bridged through oxygen (see Fig. 1). Within the rings are the two Na^+ cations. Not surprisingly, the stereo-active lone pair on the Se^{4+} points towards the Na^+ cations. The rings stack along the [100] direction, but are connected along the [010] and [001] directions (see Fig. 2). In connectivity terms, Na_2SeMoO_6 can be described as a anionic framework of $\{[SeO_{3/2}]^+[MoO_{3/2}O_{3/1}]^{3-}\}^{2-}$ with charge balance retained by two Na^+ cations. Bond distances for the MoO_6 octahedra range from 1.754(2) to 2.214(2) Å. Each Mo^{6+} cation is intra-octahedrally distorted toward a face, resulting in three ‘short’ (1.754(2) Å) and three ‘long’ (2.214(2) Å) Mo–O bonds. The SeO_3 group contains three equal Se–O bonds of 1.703(2) Å. Bond valence calculations [41,42] resulted in values of 5.84 and 4.02 for Mo^{6+} and Se^{4+}, respectively.

Unlike Na_2SeMoO_6, K_2SeMoO_6 consists of discrete dimeric anionic $[Se_2Mo_2O_{12}]^{4-}$ clusters. The dimer contains two edge-shared MoO_6 octahedra that are further connected to SeO_3 groups (see Fig. 3). The dimers are separated by K^+ cations, along the [100], [010], and [001] directions (see Fig. 4). In connectivity terms, the dimers can be described as $\{[SeO_{2/2}O_{1/1}]^0[MoO_{2/1}O_{4/2}]^{2-}\}^{2-}$ anions with charge balance retained by two K^+ cations. Bond distances range from 1.732(3) to 2.376(2) and 1.653(3) to 1.736(2) Å for the Mo–O bonds and Se–O bonds, resepctively. Bond valence calculations [41,42] resulted in values of 5.84 and 4.02 for Mo^{6+} and Se^{4+}, respectively.

Unlike either Na_2SeMoO_6 or K_2SeMoO_6, Rb_2SeMoO_6 exhibits a uni-dimensional crystal structure consisting of chains of corner-shared MoO_6 octahedra that also share edges with SeO_3 groups (see Fig. 5). The chains are separated by the Rb^+ cations. Similar to Na_2SeMoO_6, the stereo-active lone pair on the Se^{4+} point towards the Rb^+ cations. In connectivity terms the chains can be formulated as $\{[SeO_{2/2}O_{1/1}]^0[MoO_{2/1}O_{4/2}]^{2-}\}^{2-}$ with charge balance retained by two Rb^+ cations. Bond distances range from 1.732(3) to 2.235(5) and from 1.647(5) to 1.718(4) Å for the Mo–O bonds and Se–O bonds, respectively. Bond valence calculations [41,42] resulted in values of 5.96 and 4.13 for Mo^{6+} and Se^{4+}, respectively.

Table 5
Bond lengths (Å) and selected bond angles (deg) of A_2SeMoO$_6$ (A = Na, K, or Rb)

Na$_2$SeMoO$_6$			
Bond lengths			
Mo	O1	2.214(2)	
Mo	O1$^{\mathrm{i}}$	2.214(2)	
Mo	O1$^{\mathrm{ii}}$	2.214(2)	
Mo	O2	1.754(2)	
Mo	O2$^{\mathrm{i}}$	1.754(2)	
Mo	O2$^{\mathrm{ii}}$	1.754(2)	
Se	O1	1.703(2)	
Se	O1$^{\mathrm{iii}}$	1.703(2)	
Se	O1$^{\mathrm{iv}}$	1.703(2)	
Na1	O1	2.573(3)	
Na1	O1	2.573(3)	
Na1	O1	2.573(3)	
Na1	O2$^{\mathrm{iii}}$	2.367(3)	
Na1	O2$^{\mathrm{viii}}$	2.367(3)	
Na1	O2$^{\mathrm{ix}}$	2.367(3)	
Na2	O1	2.433(3)	
Na2	O1$^{\mathrm{i}}$	2.433(3)	
Na2	O1$^{\mathrm{ii}}$	2.433(3)	
Na2	O2$^{\mathrm{v}}$	2.503(3)	
Na2	O2$^{\mathrm{vi}}$	2.503(3)	
Na2	O2$^{\mathrm{vii}}$	2.503(3)	
Bond angles			
O2	Mo	O2$^{\mathrm{i}}$	104.09(8)
O2	Mo	O2$^{\mathrm{ii}}$	104.09(8)
O2	Mo	O1$^{\mathrm{ii}}$	90.82(8)
O2	Mo	O1	88.16(8)
O2$^{\mathrm{i}}$	Mo	O1	157.44(8)
O2$^{\mathrm{i}}$	Mo	O1$^{\mathrm{i}}$	88.16(8)
O2	Mo	O1$^{\mathrm{ii}}$	90.82(8)
O1$^{\mathrm{i}}$	Mo	O1	72.57(8)
O1$^{\mathrm{i}}$	Mo	O1$^{\mathrm{ii}}$	72.57(8)
O1$^{\mathrm{iii}}$	Se	O1	96.85(8)
O1$^{\mathrm{iv}}$	Se	O1	96.85(8)
O1$^{\mathrm{iv}}$	Se	O1$^{\mathrm{iii}}$	96.85(8)

K$_2$SeMoO$_6$			
Bond lengths			
Mo1	O1	2.135(2)	
Mo1	O2	1.742(3)	
Mo1	O3	1.787(2)	
Mo1	O3$^{\mathrm{i}}$	2.376(2)	
Mo1	O4$^{\mathrm{i}}$	2.187(2)	
Mo1	O5	1.732(3)	
Se1	O1	1.736(2)	
Se1	O4$^{\mathrm{i}}$	1.726(3)	
Se1	O6	1.653(3)	
K1	O1$^{\mathrm{iv}}$	3.237(3)	
K1	O2$^{\mathrm{ii}}$	2.724(3)	
K1	O4$^{\mathrm{i}}$	2.866(3)	
K1	O4$^{\mathrm{ii}}$	2.842(3)	
K1	O5	2.854(3)	
K1	O5$^{\mathrm{v}}$	2.737(3)	
K1	O6$^{\mathrm{iii}}$	2.983(3)	
K1	O6$^{\mathrm{iv}}$	3.240(3)	
K2	O1	3.051(2)	
K2	O1$^{\mathrm{ix}}$	2.785(3)	
K2	O2	2.758(3)	
K2	O2$^{\mathrm{vii}}$	3.124(3)	
K2	O2$^{\mathrm{ix}}$	3.106(3)	
K2	O3$^{\mathrm{vii}}$	3.223(3)	
K2	O3$^{\mathrm{viii}}$	2.707(2)	
K2	O6$^{\mathrm{vi}}$	2.681(3)	
Bond angles			
O1	Mo1	O3$^{\mathrm{i}}$	77.61(9)
O2	Mo1	O3$^{\mathrm{I}}$	85.29(11)
O3	Mo1	O3$^{\mathrm{I}}$	77.00(11)
O4$^{\mathrm{i}}$	Mo1	O3$^{\mathrm{i}}$	78.87(9)
O5	Mo1	O1	99.06(11)
O5	Mo1	O2	103.25(12)
O5	Mo1	O3	103.89(12)
O5	Mo1	O4i	91.87(11)
O5	Mo1	O3i	170.74(11)
O4	Se1	O1	91.16(11)
O6$^{\mathrm{i}}$	Se1	O1	103.50(13)
O6$^{\mathrm{i}}$	Se1	O4	106.34(14)

Rb$_2$SeMoO$_6$			
Bond lengths			
Mo1	O1	1.770(5)	
Mo1	O1$^{\mathrm{ii}}$	2.235(5)	
Mo1	O2	2.206(4)	
Mo1	O2$^{\mathrm{i}}$	2.206(4)	
Mo1	O3$^{\mathrm{iii}}$	1.732(3)	
Mo1	O3$^{\mathrm{iv}}$	1.732(3)	
Se1	O2	1.718(4)	
Se1	O2$^{\mathrm{i}}$	1.718(4)	
Se1	O4	1.647(5)	
Rb1	O1	3.1148(7)	
Rb1	O1$^{\mathrm{xi}}$	3.1148(7)	
Rb1	O2$^{\mathrm{v}}$	2.907(4)	
Rb1	O2$^{\mathrm{vi}}$	2.907(4)	
Rb1	O3$^{\mathrm{iii}}$	2.909(4)	
Rb1	O3$^{\mathrm{vii}}$	3.048(4)	
Rb1	O3$^{\mathrm{viii}}$	3.048(4)	
Rb1	O3$^{\mathrm{ix}}$	2.909(4)	
Rb1	O4$^{\mathrm{iii}}$	2.949(6)	
Rb2	O2	3.170(4)	
Rb2	O2$^{\mathrm{x}}$	3.170(4)	
Rb2	O3	3.226(4)	
Rb2	O3$^{\mathrm{vii}}$	2.907(3)	
Rb2	O3$^{\mathrm{viii}}$	2.907(3)	
Rb2	O3$^{\mathrm{x}}$	3.226(4)	
Rb2	O4	3.2620(18)	
Rb2	O4$^{\mathrm{viii}}$	2.933(5)	
Rb2	O4$^{\mathrm{xi}}$	3.2620(18)	
Bond angles			
O1	Mo1	O1$^{\mathrm{ii}}$	166.33(7)
O2	Mo1	O1$^{\mathrm{ii}}$	77.67(15)
O2i	Mo1	O1$^{\mathrm{ii}}$	77.67(15)
O3$^{\mathrm{iii}}$	Mo1	O1	102.01(16)
O3$^{\mathrm{iii}}$	Mo1	O1$^{\mathrm{ii}}$	86.04(15)
O3$^{\mathrm{iv}}$	Mo1	O1	102.01(16)
O3$^{\mathrm{iv}}$	Mo1	O1$^{\mathrm{ii}}$	86.04(15)
O3	Mo1	O2	90.48(16)
O3	Mo1	O2$^{\mathrm{i}}$	90.48(16)
O2$^{\mathrm{i}}$	Se1	O2	93.1(3)
O4	Se1	O2	106.34(18)
O4	Se1	O2$^{\mathrm{i}}$	106.34(18)

Symmetry transformations used to generate equivalent atoms:
(i) $0.5-y, -z, -0.5+x$;
(ii) $0.5+z, 0.5-x, -y$;
(iii) z, x, y; (iv) y, z, x;
(v) $0.5-z, 1-x, -0.5+y$;
(vi) $-0.5+x, 0.5-y, -z$;
(vii) $y, z, -1+x$;
(viii) $0.5-y, 1-z, -0.5+x$;
(ix) $1-x, 0.5+y, 0.5-z$;
(x) $0.5+x, 0.5-y, -z$;
(xi) $0.5+y, 0.5-z, -x$.

Symmetry transformations used to generate equivalent atoms:
(i) $1-x, 1-y, 1-z$;
(ii) $1-x, -0.5+y, 0.5-z$;
(iii) $1+x, y, z$;
(iv) $1+x, 0.5-y, 0.5+z$;
(v) $x, 0.5-y, 0.5+z$;
(vi) $x, 0.5-y, -0.5+z$;
(vii) $1-x, 1-y, -z$;
(viii) $-1+x, y, -1+z$;
(ix) $-x, 1-y, -z$.

Symmetry transformations used to generate equivalent atoms:
(i) $x, 0.5-y, z$;
(ii) $0.5+x, 0.5-y, 0.5-z$;
(iii) $1.5-x, -y, 0.5+z$;
(iv) $1.5-x, 0.5+y, 0.5+z$;
(v) $-0.5+x, y, 0.5-z$;
(vi) $-0.5+x, -0.5-y, 0.5-z$;
(vii) $1-x, -y, -z$;
(viii) $1-x, -0.5+y, -z$;
(ix) $1.5-x, -0.5+y, 0.5+z$;
(x) $x, -0.5-y, z$;
(xi) $x, -1+y, z$

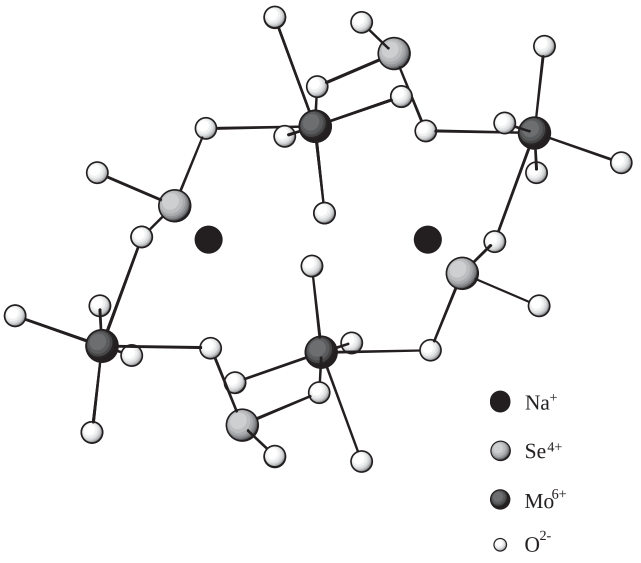

Fig. 1. Ball-and-stick diagram of the eight-membered ring in Na_2SeMoO_6 indicating the alternation between the MoO_6 octahedra and SeO_3 groups. Note that the stereo-active lone pair on the SeO_3 group point towards the Na^+ cations.

Even though all three materials have very different crystal structures, the local coordination of the cations is very similar. In all three materials the Mo^{6+} cation is in a similarly distorted octahedral environment, surrounded by six oxygen atoms. The intra-octahedral distortion is toward the face of the octahedron, and results in the three 'short' and three 'long' Mo–O bonds (see Fig. 6). In the reported materials, these distances range from 1.732(3)–1.787(2) and 2.135(2)–2.376(2) Å for the 'short' and 'long' Mo^{6+}–O bonds, respectively. This type of distortion, i.e., a 'C_3' distortion, has been observed in other Se^{4+}–Mo^{6+} oxides, namely $A_2(MoO_3)_3SeO_3$ ($A = NH_4^+$ or Cs^+) [34] and $BaMoO_3SeO_3$ [35]. Also common to A_2SeMoO_6 (A = Na, K, or Rb) is the manner in which the SeO_3 polyhedron links to the MoO_6 octahedron. In each material, it is one or more of the 'long' Mo–O bonds that links to the Se^{4+} cation. For example in Na_2SeMoO_6, Mo^{6+} is bonded to six oxygen atoms, three at a distance of 1.754(2) Å (short) and three at a distance of 2.214(2) Å (long). The oxygen atoms with the 'long' Mo–O bonds are bonded to the Se^{4+} cations, whereas the oxygen atoms with the 'short' Mo–O bonds remain terminal. With the Se^{4+} cation, three-fold oxygen coordination is observed. In addition, with both K_2SeMoO_6 and Rb_2SeMoO_6 a very short Se–O bond is observed, ~1.65 Å (see Table 5). Not surprisingly, for both materials, this bond is terminal.

Given the vastly different structural topologies, a comment must be made regarding the alkali–metal coordination. As expected, the coordination number increases from six- to eight- to nine-fold as one progresses from Na^+ to K^+ to Rb^+. In Na_2SeMoO_6,

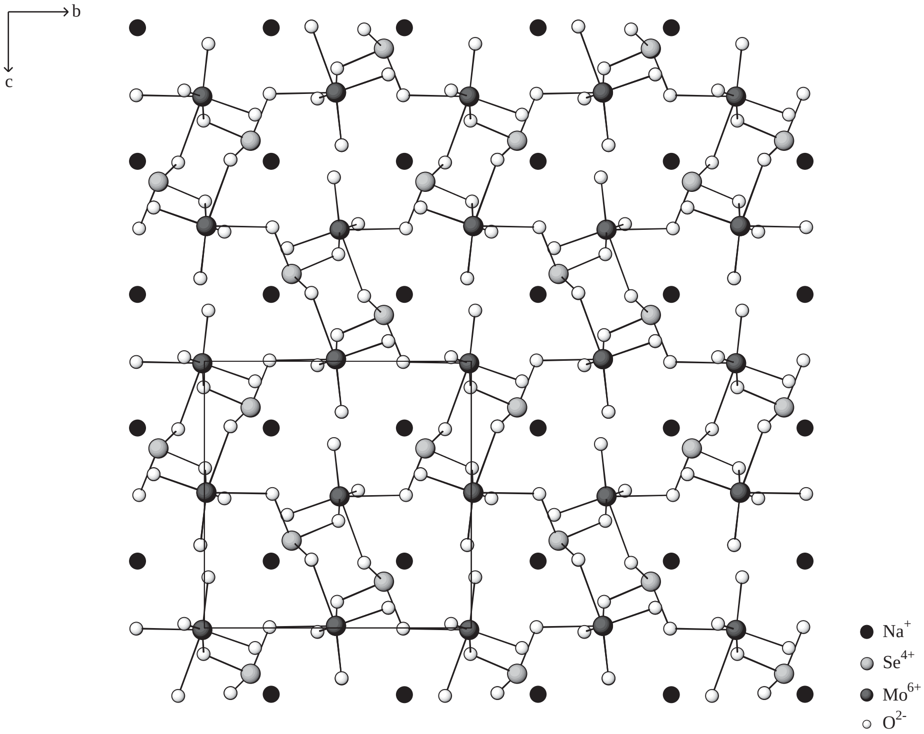

Fig. 2. Ball-and-stick diagram of Na_2SeMoO_6. The eight-membered rings are connected along the *b*- and *c*-axis.

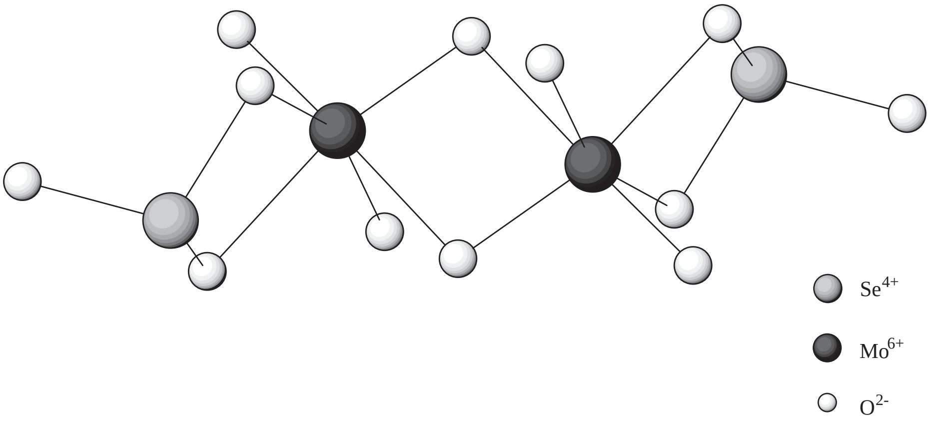

Fig. 3. Ball-and-stick diagram of the $[Se_2Mo_2O_{12}]^{4-}$ dimer in K_2SeMoO_6, showing the edge-shared MoO_6 octahedra linked to the SeO_3 groups.

the Na^+ cations are in an octahedral environment, surrounded by six oxygen atoms. The coordination environments are somewhat irregular with three 'short' and three 'long' Na–O contacts (the 'irregularity' is small compared with the aforementioned Mo–O bonds). Interestingly, the 'short' Na–O contacts for Na(1) (Na(1)–O(2): 2.367(3) Å × 3) are the 'long' Na–O contacts for Na(2) (Na(2)–O(2): 2.503(3)Å × 3). A similar situation occurs with the Na(1)–O(1) and Na(2)–O(1) interactions. With K_2SeMoO_6 and Rb_2SeMoO_6, the K^+ and Rb^+ cations are in irregular eight- and nine-fold coordination environments. The bond distances range from 2.681(3) to 3.240(3) and 2.907(3) to 3.260(2) Å for K^+ and Rb^+, respectively. It may be argued that the larger ionic radii of K^+ and Rb^+ compared to Na^+, 1.51, 1.63, and 1.02 Å, respectively, [43] results in the formation of lower dimensional structures. However, at present it is unclear why with the largest alkali cation, Rb^+, a uni-dimensional structure is observed, whereas with a smaller cation, K^+, a zero-dimensional (molecular) structure is formed.

4. Infrared spectroscopy

Infrared spectra for Na_2SeMoO_6 and K_2SeMoO_6 revealed Se–O and Mo–O stretches in the ranges of 810–904 and 768–710 cm^{-1}, respectively. In addition, several

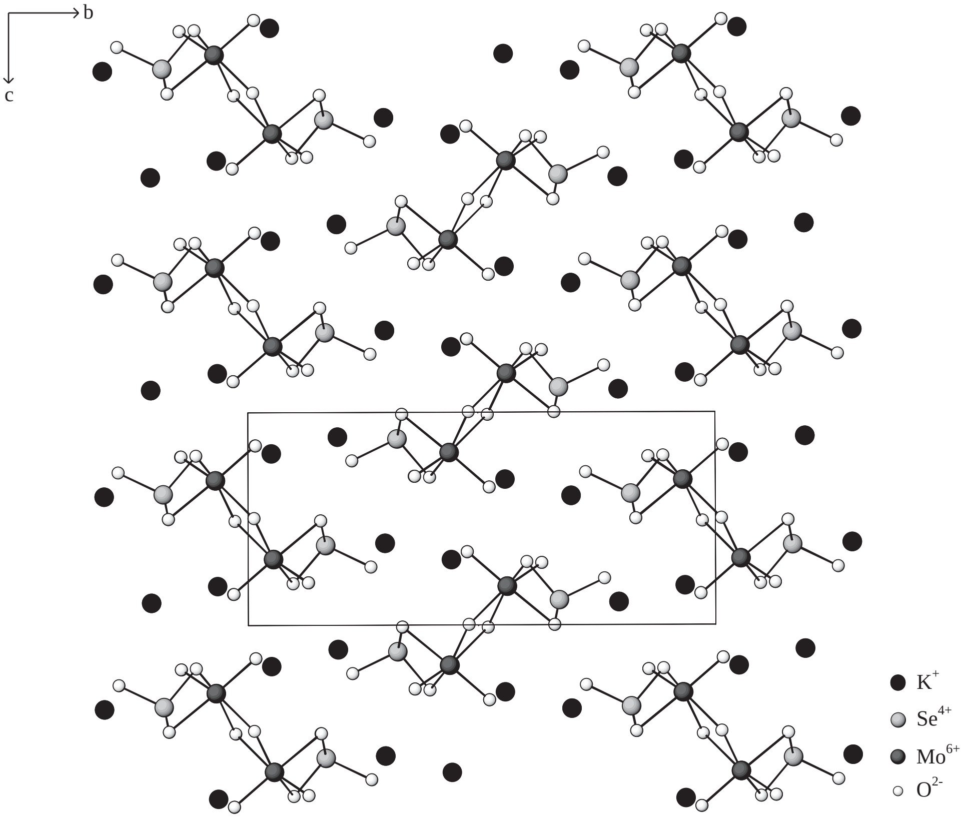

Fig. 4. Packing diagram in the $b-c$ plane for K_2SeMoO_6.

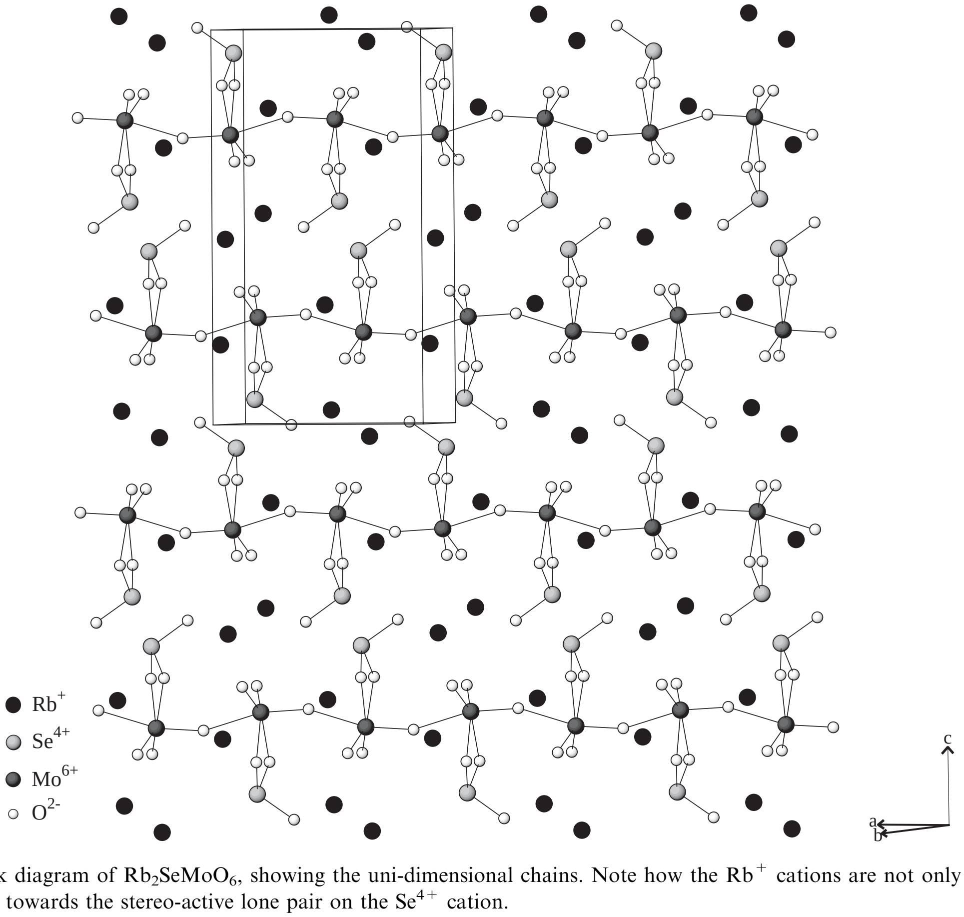

Fig. 5. Ball-and-stick diagram of Rb_2SeMoO_6, showing the uni-dimensional chains. Note how the Rb^+ cations are not only separate the chains, but are also directed towards the stereo-active lone pair on the Se^{4+} cation.

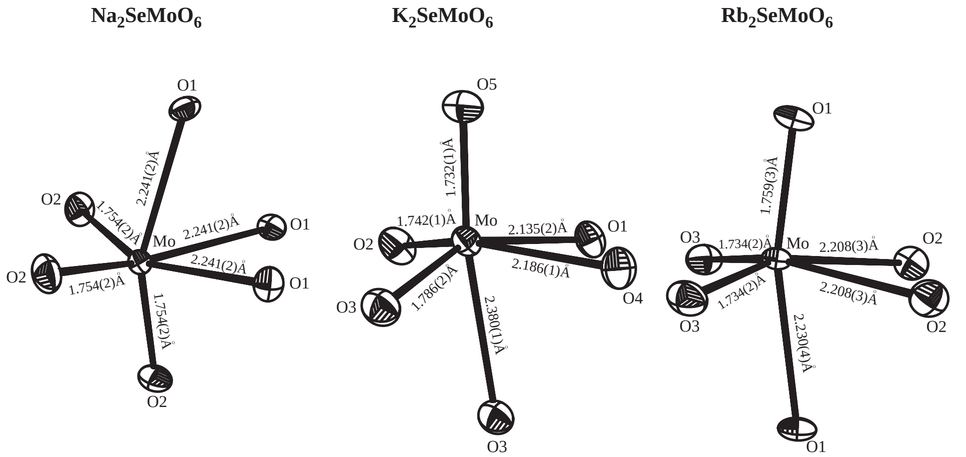

Fig. 6. ORTEP (50% probability ellipsoids) diagram of the MoO_6 octahedra in A_2SeMoO_6 ($A = Na^+$, K^+, or Rb^+). Note that in each material, the Mo^{6+} distorts in the local C_3 direction resulting in three short and three long Mo–O bonds.

Se–O–Mo and Mo–O–Mo vibrations were observed between 420 and 600 cm^{-1} for both materials. All of these stretches are consistent with those reported earlier [44,45].

5. Thermogravimetric measurements

The TG data for Na_2SeMoO_6 and K_2SeMoO_6 were very similar. Both materials lose SeO_2 over a broad temperature range (350–770°C) resulting in weight losses of 35.62% (obs.) 35.02% (calc.) and 31.22% (obs.) 31.79% (calc.) for Na_2SeMoO_6 and K_2SeMoO_6, respectively. For Na_2SeMoO_6 and K_2SeMoO_6, the remaining material was evaluated by powder X-ray diffraction and shown to be Na_2MoO_4 or K_2MoO_4, respectively [46,47].

6. Second-harmonic generation measurements

As Na_2SeMoO_6 is non-centrosymmetric, powder SHG measurements were performed. We determined that Na_2SeMoO_6 has an SHG efficiency of approximately $10 \times SiO_2$. The SHG intensity can be attributed to the polarizations coming from the SeO_3 and MoO_6 groups. This efficiency results in a $\langle d_{\text{eff}} \rangle_{\text{exp}}$ of 1.3 pm/V. By using bond hyperpolarizability (β's) values of $150 \times 10^{-40}\,m^4/V$ for Se–O and $300 \times 10^{-40}\,m^4/V$ for Mo–O and utilizing a methodology previously published [29], we determined $\langle d_{\text{eff}} \rangle_{\text{calc}} = 7.1$ pm/V for Na_2SeMoO_6.

Acknowledgments

We thank the Robert A. Welch Foundation for support. This work was also supported by the NSF-Career Program through DMR-0092054 and an acknowledgment is made to the donors of The Petroleum Research Fund, administered by the American Chemical Society, for partial support of this research. P.S.H. is a Beckman Young Investigator.

References

[1] L.E. Orgel, J. Chem. Soc. (1959) 3815.
[2] G. Meunier, J. Galy, Acta Crystallogr. B 27 (1971) 602.
[3] J. Galy, G. Meunier, S. Andersson, A. Anstrom, J. Solid State Chem. 13 (1975) 142.
[4] Y. Arnaud, M.T. Averbuch-Pouchot, A. Durif, J. Guidot, Acta Crystallogr. B 32 (1976) 1417.
[5] A. Guesdon, B. Raveau, Chem. Mater. 12 (2000) 2239.
[6] U. Opik, M.H.L. Pryce, Proc. R. Soc. (London) Ser. A 238 (1957) 425.
[7] R.F.W. Bader, Mol. Phys. 3 (1960) 137.
[8] R.F.W. Bader, Can. J. Chem. 40 (1962) 1164.
[9] R.G. Pearson, J. Am. Chem. Soc. 91 (1969) 4947.
[10] R.G. Pearson, J. Mol. Struct. (Theochem.) 103 (1983) 25.
[11] R.A. Wheeler, M.-H. Whangbo, T. Hughbanks, R. Hoffmann, J.K. Burdett, T.A. Albright, J. Am. Chem. Soc. 108 (1986) 2222.
[12] H. Nikol, A. Vogler, J. Am. Chem. Soc. 113 (1991) 8988.
[13] H. Nikol, A. Vogler, Inorg. Chem. 32 (1993) 1072.
[14] M. Kunz, I.D. Brown, J. Solid State Chem. 115 (1995) 395.
[15] G.W. Watson, S.C. Parker, J. Phys. Chem. B 103 (1999) 1258.
[16] G.W. Watson, S.C. Parker, G. Kresse, Phys. Rev. B 59 (1999) 8481.
[17] J.P. Legros, J. Galy, C. R. Acad. Sci. Ser. C 286 (1978) 705.
[18] R.E. Morris, W.T.A. Harrison, G.D. Stucky, A.K. Cheetham, J. Solid State Chem. 94 (1991) 227.
[19] R.E. Morris, W.T.A. Harrison, G.D. Stucky, A.K. Cheetham, J. Solid State Chem. 94 (1991) 227.
[20] W.T.A. Harrison, G.D. Stucky, R.E. Morris, A.K. Cheetham, Acta Crystallogr. C 48 (1992) 1365.
[21] W.T.A. Harrison, G.D. Stucky, A.K. Cheetham, Euro. J. Solid State Inorg. Chem. 30 (1993) 347.
[22] R.E. Morris, A.K. Cheetham, Chem. Mater. 6 (1994) 67.
[23] A.-M. Lafront, J. Bonvoisin, J.-C. Trombe, J. Solid State Chem. 122 (1996) 130.

[24] P.S. Halasyamani, D. O'Hare, Chem. Mater. 10 (1997) 646.

[25] P.S. Halasyamani, D. O'Hare, Inorg. Chem. 36 (1997) 6409.

[26] Y. Porter, K.M. Ok, N.S.P. Bhuvanesh, P.S. Halasyamani, Chem. Mater. 13 (2001) 1910.

[27] K.M. Ok, N.S.P. Bhuvanesh, P.S. Halasyamani, Inorg. Chem. 40 (2001) 1978.

[28] K.M. Ok, N.S.P. Bhuvanesh, P.S. Halasyamani, J. Solid State Chem. 161 (2001) 57.

[29] J. Goodey, J. Broussard, P.S. Halasyamani, Chem. Mater. 14 (2002) 3174.

[30] H.-Y. Ra, K.M. Ok, P.S. Halasyamani, J. Am. Chem. Soc. (2003), in press.

[31] C. Robl, K. Haake, J. Chem. Soc. Chem. Commun. (1992) 1786.

[32] C. Robl, K. Haake, Z. Naturforsch. B 48 (1993) 399.

[33] C. Robl, K. Haake, J. Chem. Soc. Chem. Commun. (1993) 397.

[34] W.T.A. Harrison, L.L. Dussack, A.J. Jacobson, Inorg. Chem. 33 (1994) 6043.

[35] W.T.A. Harrison, L.L. Dussack, A.J. Jacobson, J. Solid State Chem. 125 (1994) 234.

[36] SAINT, Version 4.05, Siemens Analytical X-ray Systems, Inc., Madison, WI, 1995.

[37] G.M. Sheldrick, SHELXS-97, A Program for the Automatic Solution of Crystal Structures, University of Goettingen, Goettingen, Germany, 1997.

[38] G.M. Sheldrick, SHELXL-97, A Program for the Refinement of Crystal Structures, University of Goettingen, Goettingen, 1997.

[39] L.J. Farrugia, J. Appl. Crystallogr. 32 (1999) 837.

[40] S.K. Kurtz, T.T. Perry, J. Appl. Phys. 39 (1968) 3798.

[41] I.D. Brown, D. Altermatt, Acta Crystallogr. B 41 (1985) 244.

[42] N.E. Brese, M. O'Keeffe, Acta Crystallogr. B 47 (1991) 192.

[43] R.D. Shannon, Acta Crystallogr. A 32 (1976) 751.

[44] Z. Micka, M. Danek, J. Loub, B. Strauch, J. Podlahova, J. Hasek, J. Solid State Chem. 77 (1988) 306.

[45] V.P. Verma, Thermochim. Acta 327 (1999) 63.

[46] K. Okada, H. Morikawa, F. Marumo, S.I. Iwai, Acta Crystallogr. B 30 (1974) 1872.

[47] B.M. Gatehouse, P. Leverett, J. Chem. Soc. A (1969) 849.